Luminescence

DOI: 10.1002/anie.201005624

Iridium(III) Complexes of a Dicyclometalated Phosphite Tripod Ligand: Strategy to Achieve Blue Phosphorescence Without Fluorine Substituents and Fabrication of OLEDs**

Cheng-Huei Lin, Yao-Yuan Chang, Jui-Yi Hung, Chih-Yuan Lin, Yun Chi, Min-Wen Chung, Chia-Li Lin, Pi-Tai Chou,* Gene-Hsiang Lee, Chih-Hao Chang,* and Wei-Chieh Lin*

Organic light-emitting diodes (OLEDs) based on heavy transition-metal complexes are playing a pivotal role in next generation of, for example, flat panel displays and solid-state lighting.[1] The readily available, Os^{II}-, Pt^{II}-, and in particular Ir^{III}-based phosphorescence complexes grant superior advantage over fluorescent materials.[2] This is mainly due to heavy-atom-induced spin–orbit coupling, giving effective harvesting of both singlet and triplet excitons. However, tuning of phosphorescence over the entire visible spectrum still remains a challenge. Particularly, designing new materials to show higher energy, such as deep-blue emission—with an ideal $CIE_{x,y}$ coordinate (CIE = Commission Internationale de L'Eclairage) of (0.14, 0.09)—encounters more obstacle than the progress made for obtaining green and red colors. Representative blue phosphors are a class of Ir^{III} complexes possessing at least one cyclometalated 4,6-difluorophenyl pyridine {(dfppy)H} ligand, known as FIrpic, FIr6, FIrtaz, and others.[3] The majority of blue phosphors showed inferior color chromaticity with a sum of CIE_{x+y} values being much greater than 0.3 or with single CIE_y coordinate higher than 0.25.[4] Such inferior chromaticity, in part, has been improved upon adoption of carbene-,[5] triazolyl-,[6] and fluorine-substituted bipyridine (dfpypy) based chelates.[7]

The above urgency prompted us to search for better and new blue phosphors. We produced a class of 2-pyridylazolate chelates possessing very large ligand-centered π–π* energy gap, as evidenced by the blue-emitting Os^{II} complexes.[8] Subsequently, room-temperature blue phosphorescence was also visualized for the respective heteroleptic Ir^{III} complexes,[9] particularly for those dubbed "nonconjugated" ancillary chelate(s). The nonconjugated ligands so far comprise a benzyl substituted pyrazole,[10] an N-heterocyclic carbene,[11] phosphines,[12] and other ingenious molecular designs.[13]

Herein, we report the preparation of a novel class of heteroleptic Ir^{III} complexes by incorporation of tripodal, facially coordinated phosphite (or phosphonite),[14] denoted as the P^C_2 chelate, for serving as the ancillary, together with the employment of 2-pyridyltriazolate acting as blue chromophore.[15] The reaction intermediate, which possesses an acetate chelate, was isolated and characterized to establish the synthetic pathway. The tridentate P^C_2 ancillary chelate offers several advantages: 1) Good stabilization of complex and necessary long-term stability in application of for example, emitting devices. 2) The strong bonding of phosphorous donors is expected to destabilize the ligand field d–d excited state, thus minimizing its interference to the radiative process from the lower lying excited state. 3) P^C_2 inherits profound and versatile functionality (see below) capable of fine-tuning the electronic character. As a result, highly efficient blue phosphorescence is attained with good OLED performance.

Treatment of a mixture of $[IrCl_3(tht)_3]$ (tht = tetrahydrothiophene) with an equimolar amount of triphenylphosphine (PPh_3), triphenylphosphite {$P(OPh)_3$}, and an excess of sodium acetate resulted in a high yield conversion (> 80%) into $[Ir(P^C_2)(PPh_3)(OAc)]$ (**1a**); P^C_2 = tripodal dicyclometalated phosphite (Scheme 1). Subsequent replacement of acetate in **1a** with chelating 3-*tert*-butyl-5-(2-pyridyl)triazo-

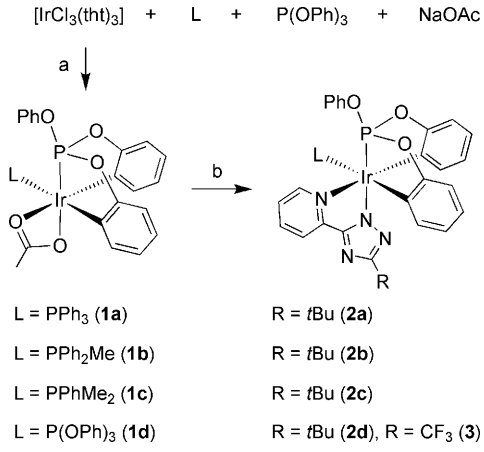

Scheme 1. Synthesis of Ir complexes **1**–**3**. Reaction conditions: a) 190 °C, 6 h; b) 190 °C, 12 h.

[*] C.-H. Lin, Y.-Y. Chang, J.-Y. Hung, C.-Y. Lin, Prof. Y. Chi
Department of Chemistry, National Tsing Hua University
Hsinchu, Taiwan 30013 (R.O.C.)
E-mail: ychi@mx.nthu.edu.tw
M.-W. Chung, C.-L. Lin, Prof. P.-T. Chou, Dr. G.-H. Lee
Department of Chemistry, National Taiwan University
Taipei, Taiwan 10617 (R.O.C.)
E-mail: chop@ntu.edu.tw
Prof. C.-H. Chang, W.-C. Lin
Department of Photonics Engineering, Yuan Ze University
Chungli, Taiwan 32003 (R.O.C.)
E-mail: chc@saturn.yzu.edu.tw

[**] This research was supported by the National Science Council (NSC-98-3114-E-007-005). OLED = organic light-emitting diode.

Supporting information for this article is available on the WWW under http://dx.doi.org/10.1002/anie.201005624.

late (bptz) gave the blue-emitting phosphor [Ir(P^C_2)(PPh_3)-(bptz)] (**2a**) in high yield (ca. 60%). After establishing the reaction protocol, for convenience and cost reduction, we prepared the analogous compounds **2b–d** and **3** by employing a one-pot procedure and skipping isolation of the intermediate **1a–d**. Furthermore, addition of three equivalents of triphenyl phosphite is necessary for optimizing the synthesis of **2d** and **3**; both complexes possess dual monodentate and dicyclometalated phosphite, showing the intrinsic difference between phosphine and the stronger π-accepting phosphite. Of particular interest are those Ir^{III} complexes **2a–d** being free from fluorine substituent; the latter is known to hamper longevity of OLEDs because of the loss of fluorine atoms through unavoidable chemical degradation.[16]

Single-crystal X-ray structural determination on **1a** and **3** confirms the key feature of dicyclometalated phosphite tripod (Figures S1 and S2 in the Supporting Information). The increase of stability with dimetalation is evidenced by the significantly reduced Ir–P distance (**1a**: 2.142 Å; **3**: 2.171 Å) versus that of monodentate phosphorous donor (**1a**: 2.378 Å; **3**: 2.270 Å) as well as the slightly less idealistic P-Ir-C bite angles of approximately 79° associated with the P^C_2 motif. Moreover, upon forming **2a–d** and **3**, the facial configuration was observed for all anionic and neutral fragments, which are represented by the cyclometalated phenyl and triazolate fragments, and the nitrogen and phosphorous donors, respectively. This configuration is evidently driven by the thermodynamic factors.

Figure 1 and Table 1 show the absorption and emission spectral data of complexes **2a–d** and **3** in degassed CH_2Cl_2. As supported by the frontier orbital analyses (see Figure S3 and Table S2), taking **2a**, **2d**, and **3**, for example, it is reasonable to assign the lower-lying absorption band around 325 nm ($\varepsilon \approx 6$–$8\times10^3\,M^{-1}cm^{-1}$) for **2a–d** and 310 nm for **3** to mainly the $\pi\rightarrow\pi^*$ transition from the cyclometalated phenyl (P^C_2) to pyridyl fragment, that is, ligand to ligand charge transfer (LLCT), overlapping in part with the Ir^{III} $d_\pi\rightarrow$pyridyl (π^*) metal to ligand charge transfer (MLCT) in the singlet manifold. Attempts to assign higher-lying electronic states were discouraged because of their complicated shapes and hence any corresponding assignments may be meaningless. Owing to the strong spin–orbit coupling, induced by the Ir^{III} metal center, a nonnegligible absorption cross section for lower-lying triplet transition is expectable on the red edge, as evidenced by the small but discernible absorption shoulder around 350–380 nm.

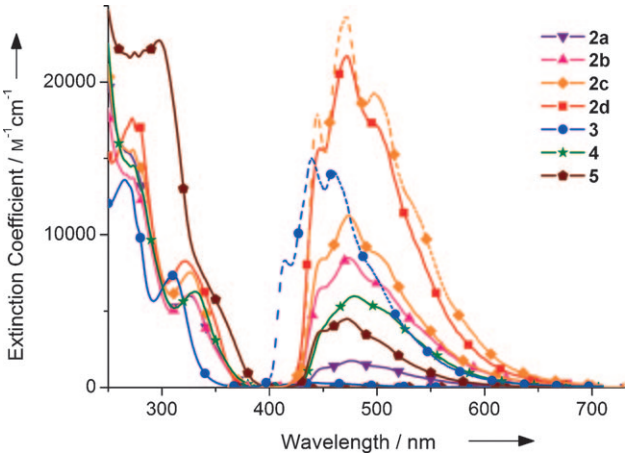

Figure 1. Absorption and luminescence spectra of **2a–2d** and **3–5** in degassed CH_2Cl_2 at room temperature (solid lines). Emission spectra of **2c** and **3** in the solid state (dashed lines). The emission scale is arbitrary, and spectra are plotted so that possible overlap between peak profiles is avoided.

Independent of types of monodentate phosphine, complexes **2a–d** exhibit blue emission with similar vibronic peak profiles at 450, 473, and 498 nm, while CF_3-substituted **3** shows significantly blue-shifted photoluminescence, with vibronic progression resolved at 416, 442, and 458 nm, corresponding to a true-blue emission with $CIE_{x,y}$ coordinate of 0.157, 0.130. For another representative example, intense phosphorescence of **2d** was observed, as indicated by its quantum yield (Φ) of as high as 0.87 in degassed CH_2Cl_2 solution at room temperature. From this result, in combination with an observed lifetime $\tau_{obs} = 44.5$ μs, we can deduce a radiative lifetime of $\tau_r = 51$ μs. Conversely, the quantum yield of **3** is exceedingly lower than that of **2d**. With an observed lifetime of 244 ns, the radiative lifetimes was deduced to be 20.3 μs. Both long radiative lifetime ($\gg 10$ μs) and vibronic feature of the phosphorescence confirms their dominant $^3\pi$–π^* nature. The major difference in quantum yields among these Ir^{III} complexes results from the different nonradiative decay rate constant k_{nr}, which is deduced to be as small as $3.00\times10^3\,s^{-1}$ for **2d** but as large as $4.09\times10^6\,s^{-1}$ for **3**. The difference in k_{nr} values among the titled complexes is of fundamental interest and may be rationalized by the systematic variation of bond strength of monodentate phosphine. Replacing PPh_3 with PPh_2Me and $PPhMe_2$ (better σ donor)

Table 1: Selected photophysical properties of Ir^{III} complexes **2a–d** and **3–5** in degassed CH_2Cl_2 solution.

	Abs. λ_{max} [nm] ($\varepsilon\times10^{-3}$)	Em. λ_{max} [nm]	Φ[a]	τ_{obs}[a]	k_r [s^{-1}]	k_{nr} [s^{-1}]
2a	250 (20.4), 271 (15.3), 326 (6.0)	450, 475, 492	0.07	2.5 μs	2.80×10^4	3.72×10^5
2b	250 (18.3), 273 (13.7), 325 (6.1)	450, 473, 498	0.34	11.1 μs	3.06×10^4	5.95×10^4
2c	250 (21.2), 273 (15.6), 327 (7.6)	451, 473, 498	0.45 (0.97)	14.3 μs (27.3 μs)	3.15×10^4	3.85×10^4
2d	272 (17.6), 279 (17.0), 322 (8.3)	447, 472, 492	0.87 (0.95)	44.5 μs (51.2 μs)	1.95×10^4	3.00×10^3
3	265 (13.6), 271 (13.1), 310 (7.3)	416, 442, 458	0.012	244 ns	4.89×10^4	4.09×10^6
4	272 (14.5), 329 (6.2)	454, 477, 495	0.24 ($\approx$1.0)	2.84 μs (22.3 μs)	8.36×10^5	2.68×10^5
5	250 (24.7), 297 (22.7), 353 (5.3)	448, 472, 494	0.18 (0.41)	5.88 μs (9.6 μs)	3.02×10^4	1.40×10^5

[a] Data measured in the solid state are given in parentheses.

and also $P(OPh)_3$ (better π acceptor) reduces the respective Ir–P distance, as supported by both X-ray structural analysis and theoretical calculations (see Table S2). Accordingly, stronger phosphines are able to further destabilize the metal-centered d–d excited states, thereby suppressing non-radiative decay pathways. In contrast, their radiative rate constant k_r increases with increase of electron-donating character of phosphine: PMe_2Ph (**2c**) > $PMePh_2$ (**2b**) > PPh_3 (**2a**) > $P(OPh)_3$ (**2d**), reflecting the increased MLCT participation in the lowest-lying excited states.

The proof of concept was then confirmed by a computational study, in which tuning the relatively energy gap between ^{3}MLCT/π–π* and ^{3}MC d–d states was examined. In this approach, the energy of higher-lying ^{3}MC d–d states was calculated by following the methodology illustrated by Persson and co-workers (see the Supporting Information for details).[17] Although being qualitative, the results shown in Figure 2 show a correlation between the bond strength of phosphorus donors and ^{3}MLCT/π–π* versus ^{3}MC d–d energy gap. Note that the P–Ir bond strength follows the order $P(OPh)_3 > PPhMe_2 > PPh_2Me > PPh_3$. The monodentate $P(OPh)_3$ ligand in **2d**, which renders the strongest Ir–P bonding, significantly increases the ^{3}MC d–d state, such that its relative energy is higher than that of the lowest-lying ^{3}MLCT/π–π* excited state. The large separation in energy also inhibits thermal population to the higher-lying ^{3}MC d–d state, accounting for the highest emission quantum yield for **2d** ($\Phi = 0.87$) in solution. Upon decreasing this Ir–P bond strength from **2d** to **2c**, the energy gap between ^{3}MLCT/π–π* and ^{3}MC d–d energy accordingly decreases. The order of energy level starts to reverse in **2b**, and the ^{3}MC d–d level turns out to be the lowest-lying excited state in **2a**. In other words, upon excitation of **2a**, the ^{3}MLCT/π–π*→^{3}MC→S_0 radiationless pathway is expected to be efficient,[18] accounting for its highest k_{nr} value, that is, the lowest emission quantum yield ($\Phi = 0.07$) and short observed lifetime (2.5 μs, see Table 1). Furthermore, as the substituent on the triazolate moiety in **2d** is changed from *tert*-butyl to trifluoromethyl to form **3**, the d_π orbital energy of Ir^{III} metal ion is decreased and hence ^{3}MLCT/π–π* energy increased (cf. **2d**, see Figure 2). Thus, despite the possession of the strongest Ir–P bonding, the net results also reverse the order of ^{3}MC and ^{3}MLCT/π–π* from **2d** to **3**. Again, the ^{3}MC d–d state becomes the lowest-energy excited state in **3**, resulting in dominant quenching process and hence much lower solution quantum yield ($\Phi = 0.012$) and rather short observed lifetime (244 ns).

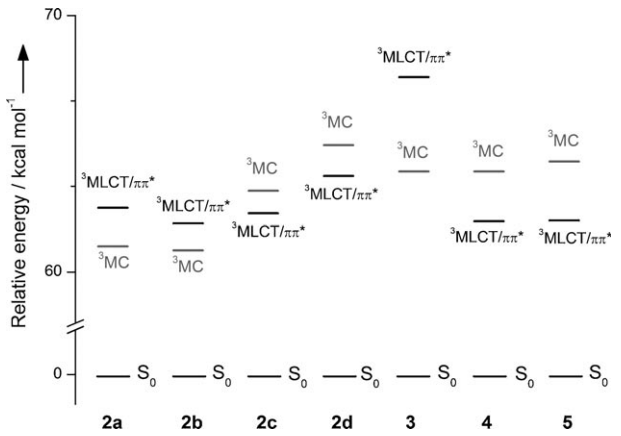

Figure 2. Energy level diagram of complexes **2a–d** and **3–5**. ^{3}MLCT/π–π* excited states were obtained from unrestricted optimization, employing X-ray structural data derived from complex **3**. The ^{3}MC d–d state was also refined by the same method, but with an initial structure derived from a distorted molecular geometry; see the Supporting Information for a detailed description. Note that the S_0 levels for all complexes are normalized.

Because of the poor emission quantum yield of **3** and insufficient volatility of **2d**, we decided to skip these phosphors, but to utilize more suitable dopant **2c** ($\Phi_p \approx 0.97$ in solid state, see Table 1) for fabrication of blue OLEDs. The as-fabricated device consist of a multilayer architecture of ITO/TAPC (30 nm)/TCTA (10 nm)/CzSi (3 nm)/CzSi doped with 4 wt% of **2c** (25 nm)/UGH2 doped with 4 wt% of **2c** (3 nm)/UGH2 (2 nm)/TmPyPB (50 nm)/LiF (0.8 nm)/Al (150 nm) (ITO = indium tin oxide, TAPC = di[4-(*N*,*N*-ditolylamino)phenyl]cyclohexane, TCTA = 4,4′,4″-tris(carbazol-9-yl)triphenylamine, CzSi = 9-(4-*tert*-butylphenyl)-3,6-bis(triphenylsilyl)-9H-carbazole, UGH2 = *p*-bis(triphenylsilyl)benzene, and TmPyPB = 1,3,5-tri[(3-pyridyl)phen-3-yl]benzene), for which configurations and structure of materials are shown in Figure S4. Notably, the wide-gap hosts CzSi and UGH2, which possess a triplet energy gap of 3.02 eV and 3.18 eV, were employed for optimal efficiency. In addition, good confinement of excitons and carriers was realized by using double emitting layers (4 wt% of dopant in both hole-transporting CzSi and electron-transporting UGH2 layers) and double buffer layers to balance the charge transport and to move the exciton-formation zone away from the adjacent carrier-transport layers. The current–voltage–luminance (*I*–*V*–*L*) characteristics and other electroluminescence performance data are depicted in Figure S5. These data are also summarized in Table 2, showing a turn-on voltage of 4.1 V, a peak external quantum efficiency (η_{ext}) of 11.0% photons per electron, a peak luminance efficiency (η_l) of 22.3 cd A^{-1}, and a peak power efficiency (η_p) of 16.7 lm W^{-1}, respectively. Upon

Table 2: Electroluminescent characteristics of blue-emitting OLEDs with different phosphors.

Device	EQE [%]		LE [cd A^{-1}]		PE [lm W^{-1}]		V_{on}[c]	Max. L [cd m^{-2}] (V [V])	CIE$_{x,y}$[b]	CIE$_{x,y}$[d]
	[a]	[b]	[a]	[b]	[a]	[b]				
2c	11.0	8.4	22.3	16.9	16.7	8.1	4.1	1431 (14.0)	0.179, 0.286	0.220, 0.336
4	8.4	8.0	17.3	16.5	13.2	8.1	4.1	6027 (13.0)	0.173, 0.303	0.185, 0.302
5	8.7	8.5	14.3	13.9	10.8	10.5	4.2	4084 (13.6)	0.169, 0.247	0.171, 0.248

[a] Maximum efficiencies. [b] Data measured at a brightness of 100 cd m^{-2}. [c] Turn-on voltage measured at 1 cd m^{-2}. [d] Data recorded at 1000 cd m^{-2}.

increasing to the practical brightness of 100 cd m^{-2}, the η_{ext}, η_l, and η_p values remain above 8.4%, 16.9 cd A^{-1}, and 8.1 lm W^{-1}, respectively, which are consistent with less significant efficiencies roll-off, and with CIE$_{x,y}$ coordinates of (0.179, 0.286).

The saturated nature of P^C$_2$ makes fine-tuning the energy gap feasible by replacing substituents on the triazolate chromophore. To demonstrate such a possibility, we synthesized the dicyclometalated diphenyl phenylphosphonite derivatives **4** and **5**, which are analogues of **2c**, to be the next generation phosphors (Scheme 2). Pertinent photophysical data for **4** and **5** are listed in Table 1. Complexes **4** and **5** all have good quantum yields in solution and the solid state ($\Phi_p \approx 1.0$ for **4**), the results of which are also consistent with the theoretical results (see Figure 2). Table 2 lists the device properties for **4** and **5** as well. Obviously, OLEDs made of either **4** or **5** achieved a three times better peak luminescence of 6027 and 4084 cd A^{-1}, and particularly for **5**, a blue CIE$_{x,y}$ color chromaticity of (0.169, 0.247). However, shifting of the CIE coordinates upon increasing the driving voltage was noted for **2c**, instead of complexes **4** and **5**. Such variation of performance may arise from the better matching of the energy levels between dopant and electron/hole transporting materials upon replacing phenoxyl (in **2c**) with phenyl fragment (in **4** and **5**), and the introduction of additional electron conducting pyridyl fragment in, for example, **5**.

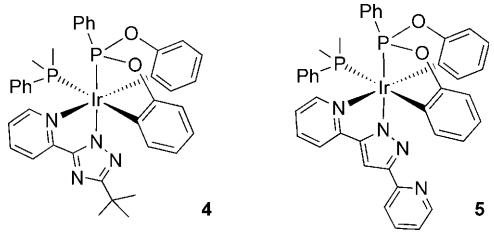

Scheme 2. Structural drawings of Ir^{III} complexes **4** and **5**.

In conclusion, we report a one-pot synthetic route to obtain a series of new blue phosphors without fluorine substituents. The molecules were assembled using dicyclometalated phosphite (or phosphonite) tripod, coupled with 2-pyridyl triazolate chromophore and a monodentate phosphorous donor. Exploiting **2c** as a paradigm, the outstanding performance includes: peak efficiencies of 11.0%, 22.3 cd A^{-1}, and 16.7 lm W^{-1}, together with a turn-on voltage of 4.1 V and blue chromaticity CIE$_{x,y}$ = 0.179, 0.286 recorded at 100 cd m^{-2}. The terdentate P^C$_2$ not only stabilizes the phosphors, its saturated nature also simplifies the color tuning strategy, as evidence by the outstanding performance of **5** toward better maximum luminescence and blue chromaticity with slight sacrifice on the peak efficiency. The results thus reveal a great potential of both P^C$_2$ and pyridyl–azolate chelates in the preparation of blue-emitting phosphors.

Received: September 8, 2010
Revised: October 15, 2010
Published online: March 1, 2011

Keywords: iridium · luminescence · N ligands · P ligands

[1] a) K. T. Kamtekar, A. P. Monkman, M. R. Bryce, *Adv. Mater.* **2010**, *22*, 572; b) Y. You, S. Y. Park, *Dalton Trans.* **2009**, 1267; c) H. Wu, L. Ying, W. Yang, Y. Cao, *Chem. Soc. Rev.* **2009**, *38*, 3391; d) W.-Y. Wong, C.-L. Ho, *J. Mater. Chem.* **2009**, *19*, 4457; e) S. Reineke, F. Lindner, G. Schwartz, N. Seidler, K. Walzer, B. Luessem, K. Leo, *Nature* **2009**, *459*, 234; f) J. A. G. Williams, S. Develay, D. L. Rochester, L. Murphy, *Coord. Chem. Rev.* **2008**, *252*, 2596; g) F. So, B. Krummacher, M. K. Mathai, D. Poplavskyy, S. A. Choulis, V.-E. Choong, *J. Appl. Phys.* **2007**, *102*, 091101; h) P.-T. Chou, Y. Chi, *Chem. Eur. J.* **2007**, *13*, 380; i) H. Wu, G. Zhou, J. Zou, C. L. Ho, W. Y. Wong, W. Yang, J. Peng, Y. Cao, *Adv. Mater.* **2009**, *21*, 4181; j) H. Sasabe, J. Takamatsu, T. Motoyama, S. Watanabe, G. Wagenblast, N. Langer, O. Molt, E. Fuchs, C. Lennartz, J. Kido, *Adv. Mater.* **2010**, *22*, 5003.

[2] a) Y. Sun, N. C. Giebink, H. Kanno, B. Ma, M. E. Thompson, S. R. Forrest, *Nature* **2006**, *440*, 908; b) B. D'Andrade, *Nat. Photonics* **2007**, *1*, 33; c) P.-T. Chou, Y. Chi, *Eur. J. Inorg. Chem.* **2006**, 3319; d) Y. Chi, P.-T. Chou, *Chem. Soc. Rev.* **2007**, *36*, 1421; e) W.-Y. Wong, C.-L. Ho, *Coord. Chem. Rev.* **2009**, *253*, 1709.

[3] a) J. Li, P. I. Djurovich, B. D. Alleyne, M. Yousufuddin, N. N. Ho, J. C. Thomas, J. C. Peters, R. Bau, M. E. Thompson, *Inorg. Chem.* **2005**, *44*, 1713; b) S.-C. Lo, G. J. Richards, J. P. J. Markham, E. B. Namdas, S. Sharma, P. L. Burn, I. D. W. Samuel, *Adv. Funct. Mater.* **2005**, *15*, 1451; c) I. Avilov, P. Minoofar, J. Cornil, L. De Cola, *J. Am. Chem. Soc.* **2007**, *129*, 8247; d) S.-J. Su, H. Sasabe, T. Takeda, J. Kido, *Chem. Mater.* **2008**, *20*, 1691; e) E. Orselli, R. Q. Albuquerque, P. M. Fransen, R. Froehlich, H. M. Janssen, L. De Cola, *J. Mater. Chem.* **2008**, *18*, 4579.

[4] a) R. J. Holmes, B. W. D'Andrade, S. R. Forrest, X. Ren, J. Li, M. E. Thompson, *Appl. Phys. Lett.* **2003**, *83*, 3818; b) Y. Zheng, S.-H. Eom, N. Chopra, J. Lee, F. So, J. Xue, *Appl. Phys. Lett.* **2008**, *92*, 223301.

[5] S. Haneder, E. Da Como, J. Feldmann, J. M. Lupton, C. Lennartz, P. Erk, E. Fuchs, O. Molt, I. Muenster, C. Schildknecht, G. Wagenblast, *Adv. Mater.* **2008**, *20*, 3325.

[6] S.-C. Lo, C. P. Shipley, R. N. Bera, R. E. Harding, A. R. Cowley, P. L. Burn, I. D. W. Samuel, *Chem. Mater.* **2006**, *18*, 5119.

[7] S. J. Lee, K.-M. Park, K. Yang, Y. Kang, *Inorg. Chem.* **2009**, *48*, 1030.

[8] a) P.-C. Wu, J.-K. Yu, Y.-H. Song, Y. Chi, P.-T. Chou, S.-M. Peng, G.-H. Lee, *Organometallics* **2003**, *22*, 4938; b) J.-K. Yu, Y.-H. Hu, Y.-M. Cheng, P.-T. Chou, S.-M. Peng, G.-H. Lee, A. J. Carty, Y.-L. Tung, S.-W. Lee, Y. Chi, C.-S. Liu, *Chem. Eur. J.* **2004**, *10*, 6255; c) Y.-M. Cheng, E. Y. Li, G.-H. Lee, P.-T. Chou, S.-Y. Lin, C.-F. Shu, K.-C. Hwang, Y.-L. Chen, Y.-H. Song, Y. Chi, *Inorg. Chem.* **2007**, *46*, 10276.

[9] Y. Chi, P.-T. Chou, *Chem. Soc. Rev.* **2010**, *39*, 638.

[10] Y.-H. Song, Y.-C. Chiu, Y. Chi, Y.-M. Cheng, C.-H. Lai, P.-T. Chou, K.-T. Wong, M.-H. Tsai, C.-C. Wu, *Chem. Eur. J.* **2008**, *14*, 5423.

[11] C.-F. Chang, Y.-M. Cheng, Y. Chi, Y.-C. Chiu, C.-C. Lin, G.-H. Lee, P.-T. Chou, C.-C. Chen, C.-H. Chang, C.-C. Wu, *Angew. Chem.* **2008**, *120*, 4618; *Angew. Chem. Int. Ed.* **2008**, *47*, 4542.

[12] a) Y.-C. Chiu, J.-Y. Hung, Y. Chi, C.-C. Chen, C.-H. Chang, C.-C. Wu, Y.-M. Cheng, Y.-C. Yu, G.-H. Lee, P.-T. Chou, *Adv. Mater.* **2009**, *21*, 2221; b) J.-Y. Hung, Y. Chi, I.-H. Pai, Y.-M. Cheng, Y.-C. Yu, G.-H. Lee, P.-T. Chou, K.-T. Wong, C.-C. Chen, C.-C. Wu, *Dalton Trans.* **2009**, 6472.

[13] Y.-C. Chiu, Y. Chi, J.-Y. Hung, Y.-M. Cheng, Y.-C. Yu, M.-W. Chung, G.-H. Lee, P.-T. Chou, C.-C. Chen, C.-C. Wu, H.-Y. Hsieh, *ACS Appl. Mater. Int.* **2009**, *1*, 433.

[14] a) E. Singleton, E. Van der Stok, *J. Chem. Soc. Dalton Trans.* **1978**, 926; b) R. B. Bedford, P. A. Chaloner, P. B. Hitchcock, *J. Chem. Soc. Chem. Commun.* **1995**, 2049; c) R. B. Bedford, S.

Castillon, P. A. Chaloner, C. Claver, E. Fernandez, P. B. Hitchcock, A. Ruiz, *Organometallics* **1996**, *15*, 3990.
[15] a) Y.-C. Chiu, C.-H. Lin, J.-Y. Hung, Y. Chi, Y.-M. Cheng, K.-W. Wang, M.-W. Chung, G.-H. Lee, P.-T. Chou, *Inorg. Chem.* **2009**, *48*, 8164; b) J.-Y. Hung, C.-H. Lin, Y. Chi, M.-W. Chung, Y.-J. Chen, G.-H. Lee, P.-T. Chou, C.-C. Chen, C.-C. Wu, *J. Mater. Chem.* **2010**, *20*, 7682.
[16] V. Sivasubramaniam, F. Brodkorb, S. Hanning, H. P. Loebl, V. van Elsbergen, H. Boerner, U. Scherf, M. Kreyenschmidt, *J. Fluorine Chem.* **2009**, *130*, 640.
[17] M. Abrahamsson, M. J. Lundqvist, H. Wolpher, O. Johansson, L. Eriksson, J. Bergquist, T. Rasmussen, H.-C. Becker, L. Hammarström, P.-O. Norrby, B. Åkermark, P. Persson, *Inorg. Chem.* **2008**, *47*, 3540.
[18] For a general review that deals with the properties of excited states, see: P.-T. Chou, Y. Chi, M.-W. Chung, C.-C. Lin, *Coord. Chem. Rev.* **2011**, DOI: 10.1016/J.CCR.2010.12.013.

